Undiagnosed Atrial Septal Defect in the Setting of Comorbidities and Ventricular Failure: Seemingly Simple Disease with a Challenging Diagnosis

Anita Sadeghpour, MD, Han Kim, MD, and Anna Lisa Chamis, MD, *Washington, District of Columbia; and Durham, North Carolina*

INTRODUCTION

Atrial septal defect (ASD) is a common congenital heart disease with variable ages of presentation. Patients may be asymptomatic until later in life, seeking medical attention after the development of dyspnea, palpitations or arrhythmias, exercise intolerance, or syncope. A standard diagnostic evaluation for these symptoms may reveal pulmonary hypertension (PH), right ventricular (RV) enlargement, and dysfunction.[1-3]

In adults, an ASD may not be initially considered in the differential diagnosis because there is considerable overlap in symptoms and electrocardiographic abnormalities in the presence of comorbidities and ventricular dysfunction. Transthoracic echocardiography (TTE) is the first-line test for the evaluation of patients with this constellation of symptoms. However, an interatrial communication may remain undiagnosed unless there is a high index of suspicion. To exclude an atrial level shunt, imaging the interatrial septum (IAS) in multiple imaging planes, including off-axis imaging, the injection of intravenous agitated saline contrast (ASC), and more advanced cardiac imaging modalities such as transesophageal echocardiography or cardiovascular magnetic resonance imaging (CMR) are often needed. Early diagnosis of ASD is important, as life expectancy may be reduced if repair is not performed before the age of 40 years.[2-4]

Herein, we describe two adult patients presenting with dyspnea, PH, and biventricular dysfunction in whom large ASDs were not identified on standard TTE.

From the MedStar Washington Hospital Center, MedStar Health Research Institute, Washington, District of Columbia (A.S.); and Duke University Medical Center, Duke Cardiovascular MR Center, Durham, North Carolina (A.S., H.K., A.L.C.).

Keywords: Atrial septal defect, Congenital heart disease, Echocardiography, Pulmonary hypertension, Cardiac magnetic resonance

Conflicts of interest: The authors reported no actual or potential conflicts of interest relative to this document.

Reprint requests: Anita Sadeghpour, MD, MedStar Washington Hospital Center, MedStar Health Research Institute, Washington, DC 20010. (E-mail: *anita.sadeghpour@medstar.net*).

2468-6441

https://doi.org/10.1016/j.case.2022.09.010

CASE PRESENTATIONS

Case 1

A 54-year-old man presented for an outpatient workup of exacerbation of shortness of breath, with a medical history of cigarette smoking, asthma, remote pulmonary emboli, and presumed alcohol-related cardiomyopathy. Prior TTE reportedly showed severe left ventricular (LV) dysfunction and PH. At the time of presentation, the patient was being treated with guideline-directed medical therapy for nonischemic cardiomyopathy, mixed-etiology PH, and pulmonary emboli.

On physical examination, the patient had no acute distress, blood pressure was 150/100 mm Hg, heart rate was 94 beats/min, and oxygen saturation on pulse oximetry was 97%. The physical examination was unremarkable and was without signs or symptoms of right-sided heart failure, cyanosis, or clubbed fingers. The 12-lead electrocardiogram showed normal sinus rhythm, biatrial enlargement, and an intraventricular conduction delay (Figure 1).

Standard TTE was performed (Videos 1-4) and showed mild LV enlargement with severely reduced systolic function and an LV ejection fraction (LVEF) of 30% by the modified Simpson method. The right ventricle was moderately enlarged, with severely reduced systolic function (tricuspid annular plane systolic excursion 23 mm, fractional area change 28%; (Figures 2 and 3). There was moderate tricuspid regurgitation, with an estimated RV systolic pressure of 45 mm Hg.

The patient underwent CMR for the evaluation of presumed nonischemic cardiomyopathy. Similar to TTE, CMR showed mild LV enlargement with significantly reduced systolic function (LVEF 30%). There was RV enlargement with severe systolic dysfunction (RV ejection fraction 20%) associated with systolic and diastolic flattening of the interventricular septum, creating a D-shaped left ventricle suggestive of RV volume and pressure overload (Figure 4).

Unexpectedly, a large defect in the IAS consistent with large secundum ASD was identified on the four-chamber view (Figure 5, *left*), and confirmed by additional imaging of the atria (Figure 5, *right*; Video 5). An en face view of the IAS demonstrated that the defect measured 3.8 × 1.8 cm (Figure 6). There were no other associated abnormalities except a sealed tiny serpiginous tunnel-shaped midmuscular ventricular septal defect (Figure 5).

The patient underwent left and right cardiac catheterization for hemodynamic evaluation and to rule out coronary artery disease. Coronary angiography revealed nonobstructive coronary artery disease. The hemodynamic study showed elevated right-sided filling pressures and mixed etiology PH with systolic pulmonary artery pressure of 62 mm Hg, pulmonary capillary wedge pressure of 23 mm Hg, and pulmonary vascular resistance of 3.0 Wood units. The patient was

VIDEO HIGHLIGHTS

Video 1: Case 1: two-dimensional TTE, apical four-chamber view, showing RV and RA enlargement. An "echo dropout" of the IAS makes it difficult to differentiate true ASD versus parallel-beam artifactual defect.

Video 2: Case 1: two-dimensional TTE, apical two-chamber view, shows severe global LV systolic dysfunction and severe left atrial enlargement.

Video 3: Case 1: two-dimensional TTE, parasternal short-axis view, demonstrates right heart dilation and possible ASD versus artifact.

Video 4: Case 1: two-dimensional TTE, subcostal view, is suggestive of a possible defect, but image quality remained suboptimal. Note the dilated inferior vena cava and hepatic vein.

Video 5: Case 1: CMR steady-state free precession four-chamber view demonstrating severe biventricular systolic dysfunction with large secundum ASD and sealed tiny serpiginous tunnel-shaped midmuscular ventricular septal defect.

Video 6: Case 2: two-dimensional TTE, apical four-chamber view, showing severe RV enlargement with severe systolic dysfunction, abnormal interventricular septal motion, severe RA enlargement with a deviation of the IAS to the left, and small pericardial effusion. There is no visible defect in the IAS.

Video 7: Two-dimensional TTE, parasternal short-axis view, shows systolic and diastolic flattening of the interventricular septum, severe RV enlargement, hypertrophied RV free wall, and moderator band.

Video 8: Two-dimensional TTE, apical four-chamber view, with color Doppler imaging showing severe posterior directed functional mitral regurgitation, mild LV enlargement, moderate left atrial enlargement, severe RV enlargement, and systolic dysfunction.

Video 9: Two-dimensional TTE, apical four-chamber view, with color Doppler imaging showing moderate functional tricuspid regurgitation due to long-standing right-sided volume overload and chronic atrial fibrillation, severe RV enlargement, and severe systolic dysfunction, abnormal interventricular septal motion, severe RA enlargement with a deviation of the IAS to the left, and small pericardial effusion.

View the video content online at www.cvcasejournal.com.

referred to the adult congenital heart disease clinic for further treatment. Surgical repair was recommended, but the patient declined; consequently, the patient underwent heart failure guideline-directed medical therapy.

Case 2

A 56-year-old man who presented with increased shortness of breath was transferred to our center for workup of chronic thromboembolic PH, mixed-etiology PH, and right-sided heart failure. The patient had a history of long-standing persistent atrial fibrillation (on anticoagulation), type 2 diabetes mellitus, obesity, systemic arterial hypertension, and obstructive sleep apnea.

On physical examination, the patient had tachycardia, with a heart rate of 104 beats/min, blood pressure of 120/80 mm Hg, and oxygen saturation on pulse oximetry of 97%. The jugular venous pressure was markedly distended, with large V waves. A 12-lead electrocardiogram showed atrial fibrillation with right bundle branch block (Figure 7).

The patient was started on milrinone and intravenous diuretic therapy. TTE was performed (Videos 6-9) and showed normal LV size with mild systolic dysfunction (LVEF 45%). The right ventricle was severely enlarged (basal diameter 5.8 cm), with severely reduced systolic function (tricuspid annular plane systolic excursion 15 mm, fractional area change 26%). There was severe functional mitral regurgitation (vena contracta of 6.5 mm, effective regurgitant orifice area of 0.35 cm^2, and systolic flow reversal of pulmonary vein) and at least moderate functional tricuspid regurgitation (vena contracta 6 mm).

The apical four-chamber view also showed severe right atrial (RA) dilatation, with no visible defect in the IAS (Figure 8).

The patient underwent right heart catheterization as a part of the PH workup protocol, which showed a mixed picture of PH (systolic pulmonary artery pressure 70 mm Hg, pulmonary capillary wedge pressure 18 mm Hg, and pulmonary vascular resistance 2.7 Wood units). An oxygen saturation study at the right atrium suggested possible shunting at the atrial level. Consequently, CMR was requested for intra- and extracardiac shunt evaluation. CMR revealed mild LV enlargement and global systolic dysfunction (LVEF 40%). There was severe RV enlargement and systolic dysfunction associated with interventricular septum flattening in systole and diastole, consistent with RV volume and pressure overload. In addition, a large defect in the upper part of the IAS at the level of the superior vena cava (SVC) and RA junction was noted, consistent with a superior sinus venosus ASD (Figure 9).

Dedicated imaging of the pulmonary veins by CMR cine imaging and angiography identified anomalous pulmonary venous drainage of the right upper pulmonary vein into the SVC and with the right

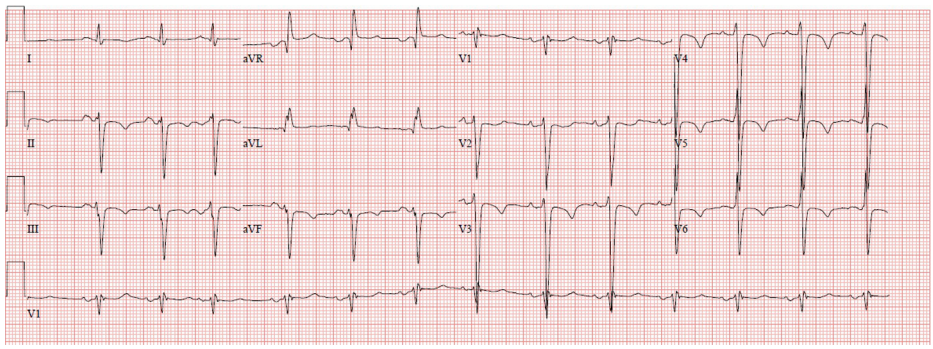

Figure 1 Twelve-lead electrocardiogram shows normal sinus rhythm, biatrial enlargement, and an intraventricular conduction delay.

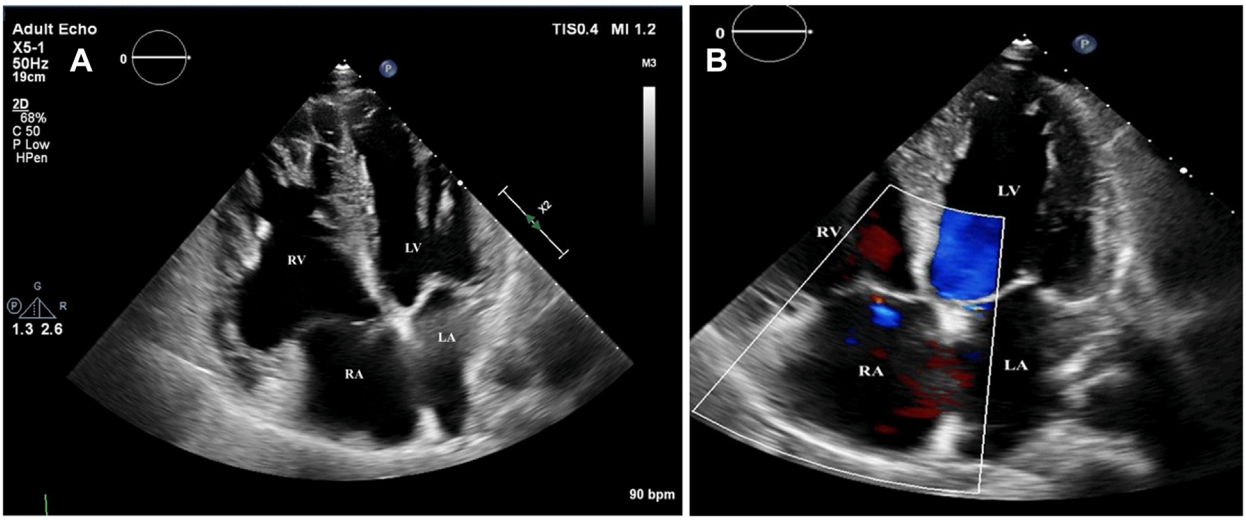

Figure 2 Apical four-chamber view by two-dimensional (*left*) and color Doppler (*right*) in mid-systole showing right ventricular and right atrial enlargement. Notice the echo dropout in the IAS. *LA*, Left atrium; *LV*, left ventricle; *RA*, right atrium; *RV*, right ventricle.

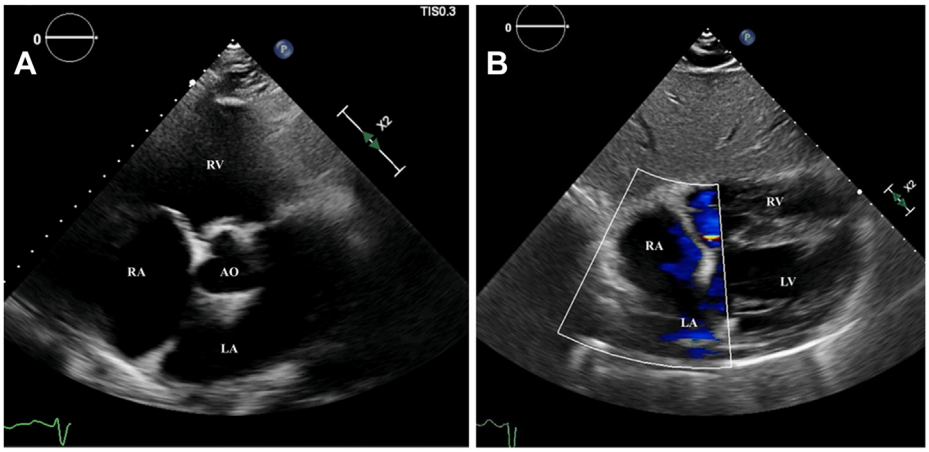

Figure 3 Parasternal short-axis view (*left*) and two-dimensional subcostal view with color Doppler imaging (*right*) in systole are suspected to depict interatrial defects. *AO*, Aorta; *LA*, left atrium; *LV*, left ventricle; *RA*, right atrium; *RV*, right ventricle.

middle pulmonary vein connecting to the SVC-RA junction (Figures 10 and 11).

The patient subsequently underwent surgical repair of the IAS communication and anomalous pulmonary venous drainage by autologous pericardial patch and baffling the anomalous pulmonary veins to the left atrium through the defect. In addition, the tricuspid and mitral valves were repaired by ring annuloplasty. The patient's symptoms had significantly diminished at the follow-up visit.

DISCUSSION

In adults, ASDs account for 30% to 40% of clinically important acyanotic intracardiac shunts.[2,5] Many patients remain asymptomatic in the first two decades of their lives, and if they remain undiagnosed, they may present with symptoms such as shortness of breath, fatigue, palpitation, exercise intolerance, or syncope later in life. Importantly, the rate of atrial arrhythmia and the morbidity and mortality of patients with unrepaired ASDs significantly increase in patients older than 40 years.[1,2,5]

Different types of ASDs have been defined on the basis of the location of the defect. Septum secundum ASD is the most common type (60%-80%), with a true defect in the region of fossa ovalis, followed by the primum ASD (15%-20%), which is also known as a partial atrioventricular septal defect and almost always involves atrioventricular valves including anterior mitral leaflet cleft. The third type is sinus venous–type ASD (4%-11%), defined as communication between one or more of the right-sided pulmonary veins, atria, and vena cava overriding the IAS. Sinus venous–type ASDs are subcategorized as superior sinus venosus defects (5%) and inferior sinus venosus defects 1%.[2,6]

The potential symptoms and signs of ASD often overlap with other conditions commonly found in adults. In these instances, direct or

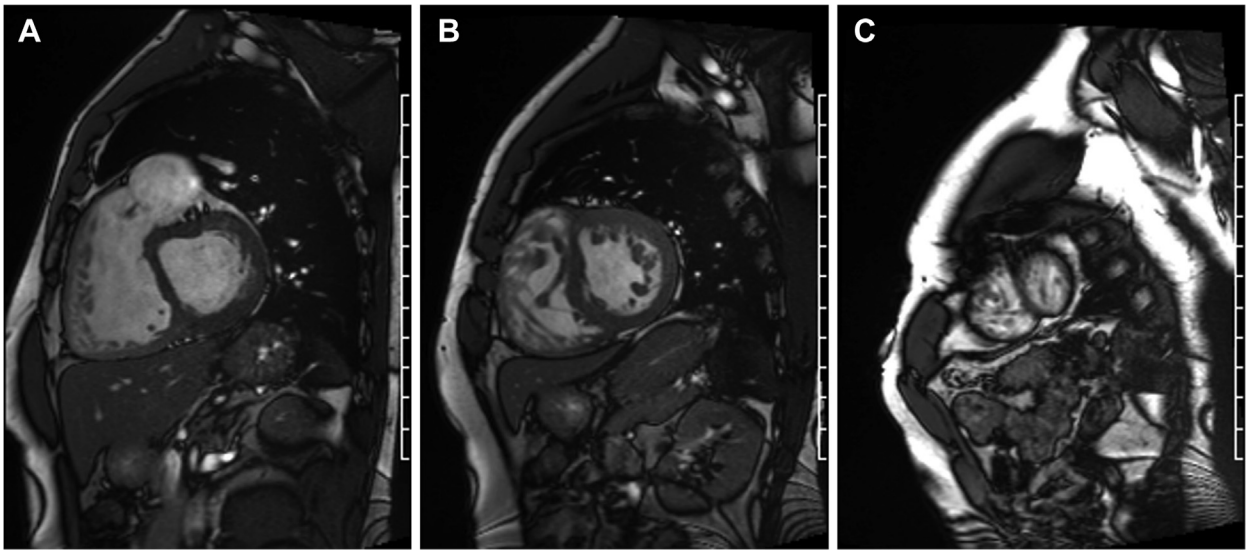

Figure 4 CMR short-axis steady-state free precession cine images of the left and right ventricles from the base (*left*), midlevel (*middle*), and apex (*right*) in the diastolic phase show significant RV enlargement with flattening of the interventricular septum, creating a D-shaped left ventricle.

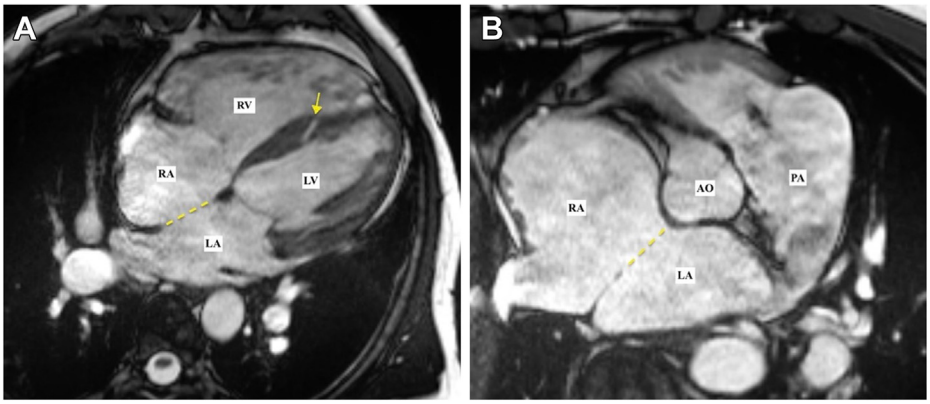

Figure 5 CMR steady-state free precession cine images in systolic phase. (*Left panel*) Four-chamber view corresponds to Video 5, with sealed tiny serpiginous tunnel-shaped midmuscular ventricular septal defect (*yellow arrow*). Short-axis view of the aortic valve (*right*) demonstrates a large secundum ASD (*dashed line*). *AO*, Aorta; *LA*, left atrium; *LV*, left ventricle; *PA*, pulmonary artery; *RA*, right atrium; *RV*, right ventricle.

indirect findings of a shunt by TTE are a pivotal step in identifying the diagnosis. However, direct visualization of atrial communications on TTE can be challenging. For example, obesity or pulmonary disease can lead to poor acoustic windows, impairing visualization of the IAS. Additionally, from the apical four-chamber view, "echo dropout" of the IAS due to parallel alignment of the ultrasound beam with the septum could lead a reader to interpret the absence of tissue in the fossa ovalis as an imaging artifact (Figures 2 and 3).

Importantly, imaging in multiple views, including the subcostal four-chamber view and off-axis imaging, can improve visualization of the IAS, as the ultrasound beam is more perpendicular to the septum.[7] Intravenous injection of ASC can help identify abnormal left-to-right shunting,[8,9] considering that ASC might be falsely negative because of insufficient RA opacification or the presence of a prominent Eustachian valve that directs inferior vena cava flow toward the IAS and prevents agitated saline bubbles in the SVC from crossing the IAS.[7] Consequently, a high index of suspicion of an ASD is required to extend the transthoracic echocardiographic examination to include these additional views and techniques.

In our first case, "echo dropout" of the IAS in the apical four-chamber view and limited subcostal images due to obesity and chronic obstructive pulmonary disease were the main limitations to diagnosing ASD. It is noteworthy that ASD shunt flow in the presence of significant PH and high RA pressure can be bidirectional or right to left, making it difficult to identify by color Doppler imaging in adult patients.[7] Also, ASC was not given, likely because of the presence of

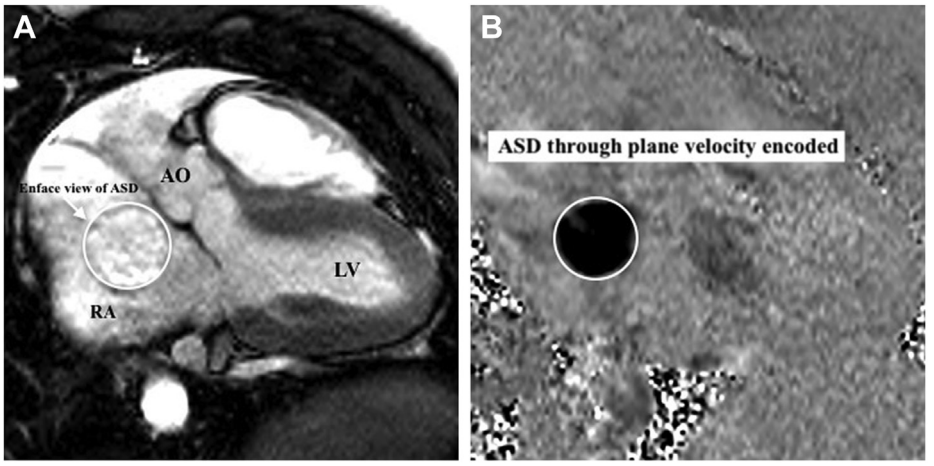

Figure 6 En face views of the IAS by CMR, steady-state free precession cine image (*left*), and through-plane velocity-encoded CMR image (*right*) in the early systolic phase demonstrating an ASD marked by the *white circle*. The en face view shows the anatomic relationship between the defect and the aortic root and allows the direct quantification of the flow through the ASD. *AO*, Aorta; *LV*, left ventricle; *RA*, right atrium.

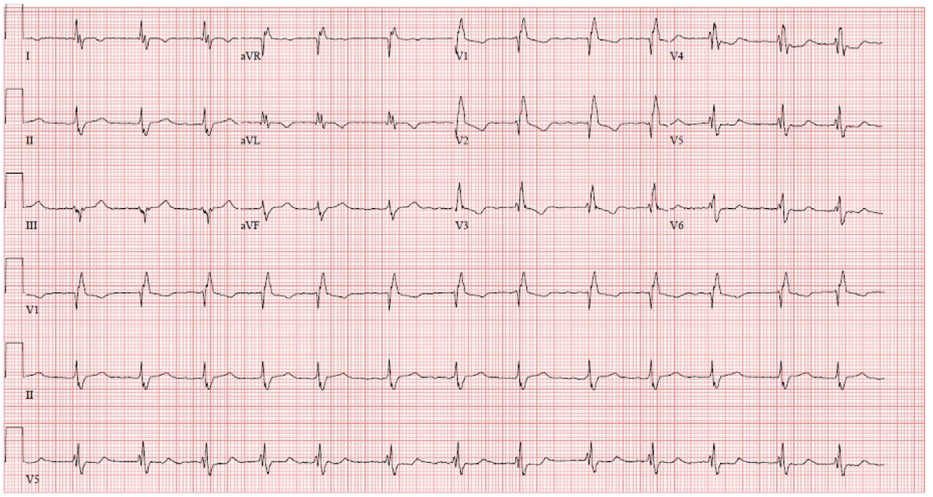

Figure 7 Twelve-lead electrocardiogram shows atrial fibrillation with right bundle branch block.

alternative explanations for right-sided enlargement and or not detecting any defect or shunt flow on TTE. We believe that having a standing protocol in the echocardiography laboratory for patients with right-sided chamber enlargement can be enormously helpful in the diagnosis of adults with ASDs. Herein we propose a standing protocol for patients with right-sided chamber enlargement to be used in echocardiography laboratories (Figure 12) to diminish the number of undiagnosed ASDs in adult patients. We believe that earlier diagnosis means proper management and a better prognosis.

In the second case, direct visualization of the sinus venosus defect was more challenging because of the superior and posterior location of the ASD. Again, injection of ASC was not considered. The identification of sinus venosus defects requires a high index of suspicion. Typically, standard TTE does not visualize the superior and posterior portion of the IAS. Even if dedicated views are performed on TTE, other cardiac imaging modalities are needed to visualize the interatrial communication (Figure 12).[9-11]

CMR may be well suited for the identification of complex ASDs. Imaging can be performed in any imaging plane, facilitating the assessment of these defects. In particular, direct en face imaging (Figure 6) provides a precise anatomic localization of the shunt within the IAS, improves the hemodynamic assessment of these shunts, and allows the visualization of even small or fenestrated defects on quick visual inspection.[12] Additionally, CMR identifies the presence of partial anomalous pulmonary venous drainage, which is commonly associated with sinus venosus ASDs and is also found in subsets (~10%-15%) of ostium secundum ASDs.[13] The presence, location, and number of anomalous pulmonary venous drainage change the therapeutic approach from percutaneous to surgical closure in most patients.[13,14]

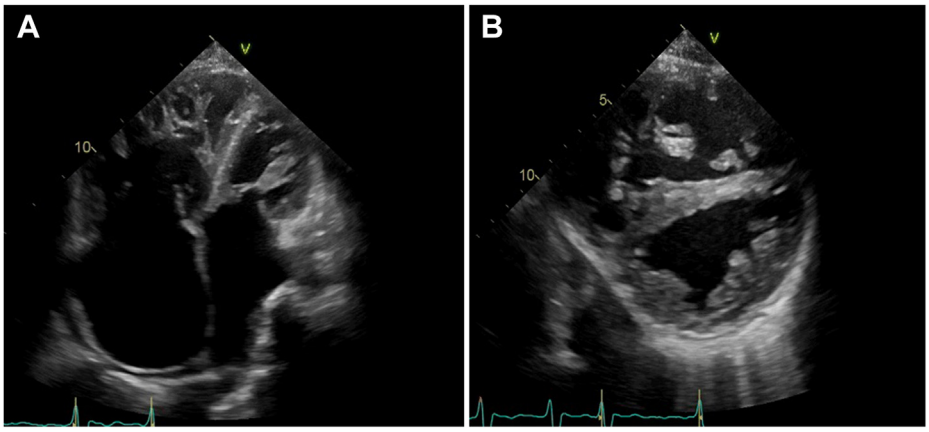

Figure 8 Apical four-chamber view (*left*) and parasternal short-axis view (*right*) showing severe RV enlargement and diastolic flattening of the interventricular septum.

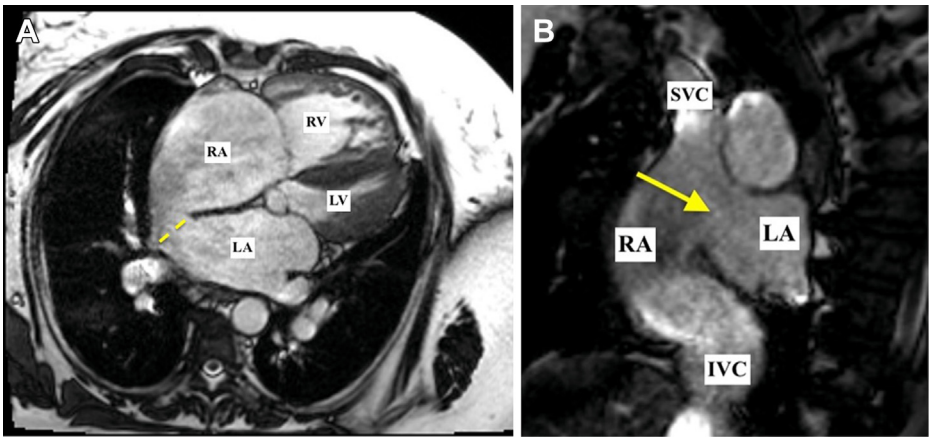

Figure 9 CMR steady-state free precession cine images in horizontal long-axis view (*left*) and sagittal oblique view (*right*) in systole demonstrate a large defect at the superior part of the IAS, consistent with a superior sinus venous ASD (*yellow dashed line and arrow*). *IVC*, Inferior vena cava; *LA*, left atrium; *LV*, left ventricle; *RA*, right atrium; *RV*, right ventricle.

In adults, ASD is an underrecognized cause of PH. The prevalence of significant PH in patients with unrepaired ASD is 10% to 34%.[15,16] Notably, Eisenmenger syndrome due to ASD accounts for 5% to 10% of all causes of pulmonary arterial hypertension.[16] TTE is a first-line test in the evaluation for PH, providing an estimate of PH probability, and is used to exclude secondary causes of PH. However, if no overt atrial-level shunt is detected on TTE, additional imaging such as transesophageal echocardiography and CMR should be strongly considered to exclude an ASD and/or partial anomalous pulmonary venous drainage.[17]

Assessment of RV systolic function by conventional echocardiographic parameters such as S′ and tricuspid annular plane systolic excursion may be misleading in the setting of significant left-to-right shunting, as they are load dependent. Three-dimensional echocardiography and two-dimensional strain as advanced echocardiographic techniques are more accurate and reproducible compared with CMR as the reference standard technique.

Even in patients with other potential explanations for PH (e.g., pulmonary emboli, in situ pulmonary thrombosis, severe obstructive lung disease), it may be reasonable to also exclude the presence of an ASD.[2,17] In both of the cases presented herein, the etiology of PH was thought to be multifactorial and was attributed to a combination of obstructive sleep apnea, thromboembolic disease, and left-sided heart failure. Interestingly, severe LV systolic dysfunction has been rarely reported in patients with ASDs and led to delays in diagnosis and treatment in our patients. In this setting, measurement of pulmonary artery flow and aortic flow by pulsed-wave Doppler can be helpful. A high pulmonary artery/aortic flow ratio is suggestive of a possible shunt and, if present, should be investigated further.[18]

CONCLUSION

The diagnosis of ASD in adults with multiple comorbidities and ventricular failure is challenging. Comprehensive TTE using multiple views (including subcostal and off-axis views), ASC injection, and having a standing protocol in the echocardiography laboratory improve the diagnosis of ASD in adults. More important, a high index of suspicion is needed to find concomitant ASDs in patients with right-sided chamber enlargement

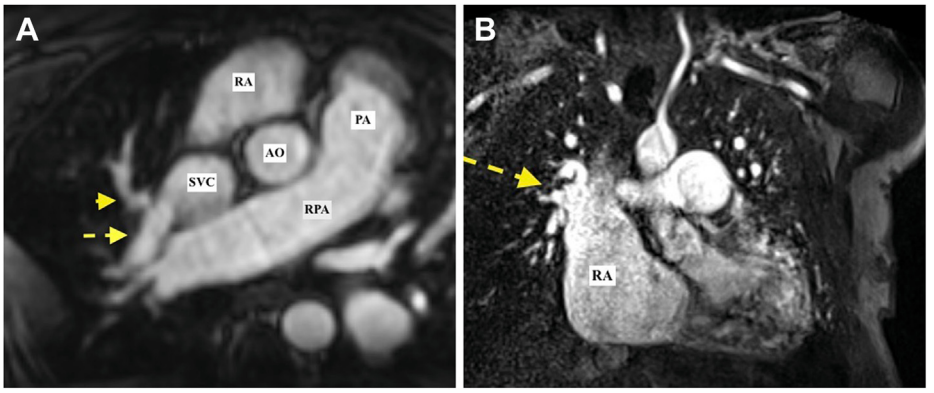

Figure 10 Right upper and middle pulmonary veins drain anomalously into the SVC as visualized on CMR, steady-state free precession axial image (*left*), and CMR, contrast-enhanced magnetic resonance angiographic coronal cut (*right*). Notice the anomalous pulmonary venous drainage to the SVC (*yellow arrows*). *AO*, Aorta; *PA*, pulmonary artery; *RA*, right atrium; *RPA*, right pulmonary artery.

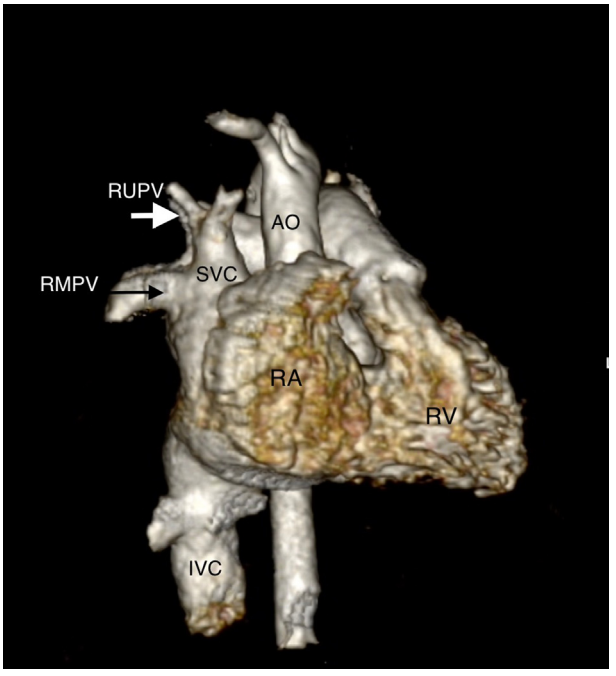

Figure 11 Three-dimensional volume-rendered image derived from CMR angiography. The right upper pulmonary vein (RUPV) anomalously drains into the SVC (*white arrow*). The right middle pulmonary vein (RMPV) anomalously drains into the junction of SVC and right atrium (RA; *black arrow*). *Ao*, Ascending aorta; *IVC*, inferior vena cava; *RV*, right ventricle.

irrespective of PH or ventricular function. Further evaluation using transesophageal echocardiography and CMR or cardiac computed tomography will confirm the presence, size, and type of the ASD and associated anomalies such as anomalous pulmonary venous connection.

ACKNOWLEDGMENT

We thank Dr. Anita Kelsey for her help in providing the diagnostic algorithm for patients with right-sided chamber enlargement referring to the echocardiography laboratory.

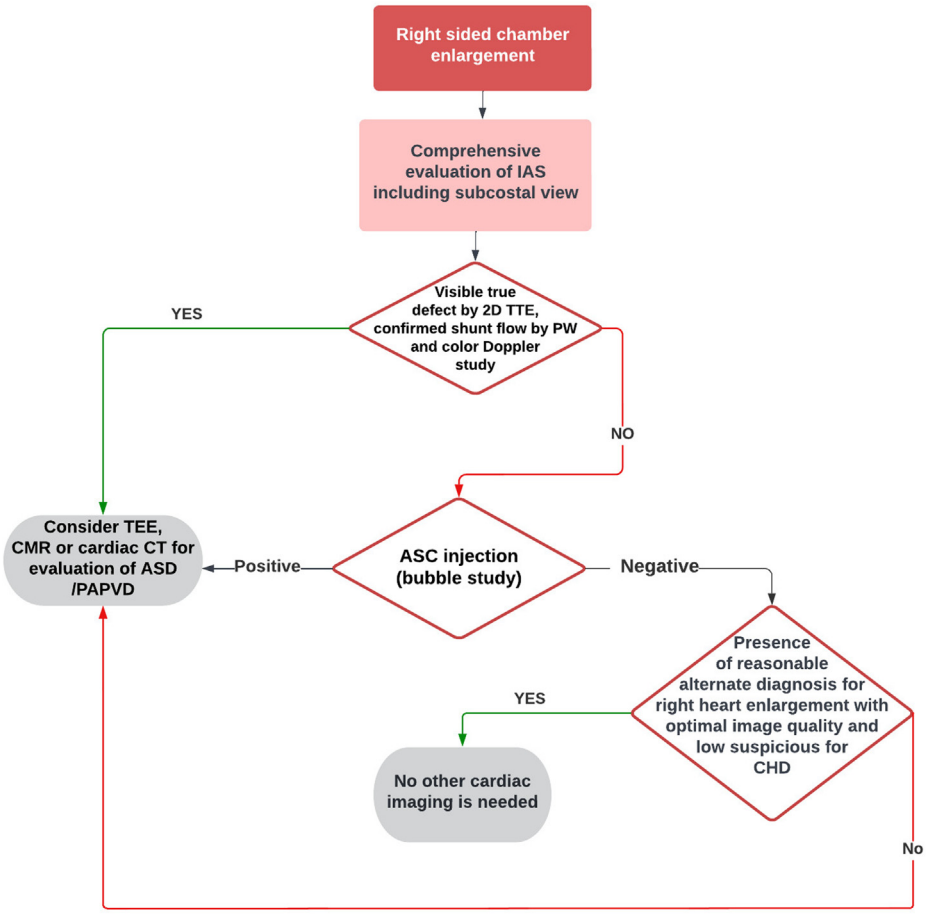

Figure 12 Diagnostic algorithm for patients referred to the echocardiography laboratory with right-sided chamber enlargement. *CDI*, Color Doppler imaging; *CHD*, congenital heart disease; *CT*, computed tomography; *PAPVD*, partial anomalous pulmonary venous drainage; *PW*, pulsed-wave; *TEE*, transesophageal echocardiography.

SUPPLEMENTARY DATA

Supplementary data related to this article can be found at https://doi.org/10.1016/j.case.2022.09.010.

REFERENCES

1. Warnes CA, Williams RG, Bashore TM, Child JS, Connolly HM, Dearani JA, et al. ACC/AHA 2008 guidelines for the management of adults with congenital heart disease. J Am Coll Cardiol 2008;52:e143-263.
2. Geva T, Martins JD, Wald RM. Atrial septal defects. Lancet 2014;383:1921-32.
3. Webb G, Gatzoulis MA. Atrial septal defects in the adult. Circulation 2006;114:1645-53.
4. Nyboe C, Karunanithi Z, Nielsen-Kudsk JE, Hjortdal VE. Long-term mortality in patients with atrial septal defect: a nationwide cohort-study. Eur Heart J 2017;39:993-8.
5. Therrien J, Webb G. Clinical update on adults with congenital heart disease. Lancet 2003;362:1305-13.
6. Surkova E, Babu-Narayan SV, Semple T, Ho SY, Li W. International Journal of Cardiology Congenital Heart Disease the ACHD multi-modality imaging series: imaging of atrial septal defects in adulthood. Int J Cardiol Congen Heart Dis 2021;4:100188.
7. Silvestry FE, Cohen MS, Armsby LB, Burkule NJ, Fleishman CE, Hijazi ZM, et al. Guidelines for the echocardiographic assessment of atrial septal defect and patent foramen ovale: from the American Society of Echocardiography and Society for Cardiac Angiography and Interventions. J Am Soc Echocardiogr 2015;28:910-58.
8. Bernard S, Churchill TW, Namasivayam M, Bertrand PB. Agitated saline contrast echocardiography in the identification of intra- and extracardiac shunts: connecting the dots. J Am Soc Echocardiogr 2021;34:1-12.
9. Shub C, Dimopoulos IN, Seward JB, Callahan JA, Tancredi RG, Schattenberg TT, et al. Sensitivity of two-dimensional echocardiography in the direct visualization of atrial septal defect utilizing the subcostal approach: experience with 154 patients. J Am Coll Cardiol 1983;2:127-35.
10. Yamamura D, Alexander T. A lifetime secret: congenital heart disease in the elderly. J Am Coll Cardiol 2021;77:2769.
11. Qiu JK, Bamira D, Vainrib AF, Latson LA, Halpern DG, Chun A, et al. Multimodality imaging of sinus venosus atrial septal defect: a challenging diagnosis in adults. CASE (Phila) 2022;6:107-13.
12. Thomson LE, Crowley AL, Heitner JF, Cawley PJ, Weinsaft JW, Kim HW, et al. Direct en face imaging of secundum atrial septal defects by velocity-encoded cardiovascular magnetic resonance in patients evaluated for possible transcatheter closure. Circ Cardiovasc Imaging 2008;1:31-40.
13. Sahay S, Krasuski RA, Tonelli AR. Partial anomalous pulmonary venous connection and pulmonary arterial hypertension. Respirology 2012;17:957-63.

14. Stout KK, Daniels CJ, Aboulhosn JA, Bozkurt B, Broberg CS, Colman JM, et al. 2018 AHA/ACC guideline for the management of adults with congenital heart disease: a report of the American College of Cardiology/American Heart Association Task Force on Clinical Practice Guidelines. Circulation 2019;139:e698-800.
15. Craig RJ, Selzer A. Natural history and prognosis of atrial septal defect. Circulation 1968;37:805-15.
16. Le Gloan L, Legendre A, Iserin L, Ladouceur M. Pathophysiology and natural history of atrial septal defect. J Thorac Dis 2018;10:S2854-63.
17. Galiè N, Humbert M, Vachiery J-L, Gibbs S, Lang I, Torbicki A, et al. 2015 ESC/ERS guidelines for the diagnosis and treatment of pulmonary hypertension: the Joint Task Force for the Diagnosis and Treatment of Pulmonary Hypertension of the European Society of Cardiology (ESC) and the European Respiratory Society (ERS): endorsed by: Association for European Paediatric and Congenital Cardiology (AEPC), International Society for Heart and Lung Transplantation (ISHLT). Eur Heart J 2015;37:67-119.
18. Ennezat PV, Juthier F, Maréchaux S, Mouquet F, Bauchart JJ, Auffray JL, et al. Atrial septal defect associated with dilated cardiomyopathy in the setting of acute cardiac failure: importance of comprehensive bedside echocardiography in ICU. Eur J Echocardiogr 2009;11:E11.